

---

# Measurement and Estimation of Organ Bremsstrahlung Radiation Dose

Lawrence E. Williams, Jeffrey Y. C. Wong, David O. Findley\*, and Bruce W. Forell

*Divisions of Radiology and Radiation Oncology at the City of Hope National Medical Center, Duarte, California*

Bremsstrahlung radiation doses were measured in an anthropomorphic phantom using thermoluminescent dosimeters. A single source of  $^{90}\text{Y}$  (beta-ray range  $\leq 1.0$  cm) was inserted in the bladder region and dosimeters were placed at distances  $\geq 3$  cm to preclude detection of decay betas. Doses were corrected so as to represent the case of no biologic clearance. By comparing dosimeter location with the standard MIRD human geometry, sample organ doses could be determined. Representative results were  $432 \pm 76$  mrad/mCi at 3 cm (bladder),  $260 \pm 60$  mrad/mCi (uterus),  $71 \pm 4$  mrad/mCi (lower large intestine), and  $1.4 \pm 0.7$  mrad/mCi (liver). An estimation method, based on absorbed fraction tables, gave organ doses that were within the errors of measurement for all tissues with the exception of the bladder site. We conclude that organ bremsstrahlung radiation doses are not negligible and that they can be estimated using an integration over both the brake and beta-ray spectra.

J Nucl Med 30:1373-1377, 1989

---

**B**remsstrahlung (brake radiation) is the continuous spectrum of x-rays produced when electrically charged particles are decelerated during their passage through an absorbing medium. Estimates of the probability of bremsstrahlung production relative to that of ionization of the medium are found to be proportional to both the initial energy ( $E$ ) of the charged particle and the average atomic number of the absorber ( $\bar{Z}$ ); e.g.,  $(\bar{Z}E)/800$  in the case of the electron ( $I$ ). Such estimates are rather crude and are difficult to apply to internal organ radiation dose estimations or to radiation protection considerations. The former would be particularly true since knowledge of absorbed fractions ( $\phi$ ) of the emitted energies would also be required (2). Thus, unlike the cases of most gamma (2) or low-energy beta emitters (3), no estimates are presently available for bremsstrahlung organ dose. Scientific and ethical motivation for the development of such methods are clearly present in an era when high-energy beta sources are being considered for use in radiotherapy of cancer patients (4).

In the following, we demonstrate a technique that permits organ dosimetric predictions for bremsstrahlung

from a general beta emitter. We carry out the calculations explicitly for the representative nucleus yttrium-90 ( $^{90}\text{Y}$ ). This radionuclide, which has a maximum beta energy of 2.27 MeV and a physical half-life of 64 hr, is being used in a polyclonal antibody therapy protocol (5). It has had previous application, when bound to glass spheres, in the treatment of human pancreatic and hepatic malignancies (6, 7). When chelated to diethylenetriaminepentaacetic acid (DTPA),  $^{90}\text{Y}$  has been applied to the treatment of central nervous system malignancies (8) while a colloidal species has been reported effective in radiation synovectomy (9). Ionic forms tend to target the bone marrow and the citrate ion has been utilized in the palliative treatment of bone metastatic disease (10). Evaluation of Fermi's equality (1) for the likelihood of  $^{90}\text{Y}$  bremsstrahlung emission yields a probability of 0.81% compared with that for the production of ionization of a water medium.

Several estimates have been made of the radiation exposure rate around a small source of  $^{90}\text{Y}$  surrounded by sufficient water medium to attenuate all the emitted betas. Cember (11) has given an approach that leads to the value 2.7 mR/hr at 3 cm from a 1-mCi source. Larger values of 5.3 and 11 mR/hr can be estimated using methodologies, respectively, of Berger (12) and of the Radiological Health Handbook (13) at the same geometric position. These values differ extensively—to some degree because of the presence of the strontium-90 ( $^{90}\text{Sr}$ ) parent in the sample (13).

---

Received Oct. 21, 1988; revision accepted Feb. 28, 1989.

For reprints contact: L. E. Williams, Div. of Radiology, City of Hope National Medical Center, Duarte CA 91010.

\* Present address: Dept. of Therapeutic Radiology/Physics Section, Stanford University Medical Center, Stanford CA 94305-5105.

## MATERIALS AND METHODS

### Phantom

In order to check the dose estimation and protection calculations, it is important to measure bremsstrahlung radiation doses in geometric conditions approaching those seen in the clinic. For these purposes, we utilized the RANDO humanoid phantom which contains a human skeleton and lung equivalent material. The phantom is cut into 2.54-cm-thick transaxial sections with positions for dosimeter placement in a rectangular grid at 3-cm spacing.

### Algorithm for Brake Dose Calculation

We base our derivation on the MIRD (3) formula:

$$\text{Brake Dose (organ } j) = (\tilde{A}_k/m_j) \sum_i \Delta_i \phi_{ijk} = \tilde{A}_k S_{jk}, \quad (1)$$

where  $\Delta_i = 2.13 E'_i(\text{MeV}) n_i$  as defined by Loewinger and Berman (14). Here  $\phi_{ijk}$  is the probability of absorption of a bremsstrahlung photon of energy  $E'$  (MeV) at target organ  $j$  following its emission from source organ  $k$  and the parameter  $n_i$  represents the probability of emission of this photon. Target organ  $j$  has mass  $m_j$ . Present MIRD tabulations provide  $\phi$  as a function of  $E'_i$  and particular source and target organs (2). Cumulated activity ( $\tilde{A}$ ), the remaining parameter in Eq. (1), is defined as the integral of activity over time and has units of  $\mu\text{Ci-hr}$ .

Both  $\Delta$  and  $\phi$  depend on the energy of the bremsstrahlung photon  $E'_i$ . Suppressing the  $k$  and  $j$  indices for brevity and replacing the sum over the  $i$  index with a double integration, we rewrite Eq. (1) as the integral:

$$\text{Brake Dose} = (\tilde{A}/m) 2.13 \int_0^{E_{\max}} \int_0^E f(E') E' \phi(E') dE' dE. \quad (2)$$

Here  $f$  is defined as  $dn/dE'$ , the spectrum of brake photons. In the following, this spectrum was set equal to the product of the normalized beta spectrum  $P(E)$  times the so-called thick-target or triangular formulation (15) for the photon spectrum. The last assumption arises since the high-energy betas are stopping in sections of tissue having dimensions on the order of centimeters. Explicitly, the result was:

$$dn/dE' = P(E)[(E - E')/E'] \bar{Z} C, \quad (3)$$

with  $\bar{Z}$  being the average atomic number of the source organ beta absorber and  $C$  a constant equal to  $2.76 \times 10^{-3}$  (16). Then the  $S$  function corresponding to Eq. (2) becomes:

$$mS = 2.13 \bar{Z} C \int_0^{E_{\max}} P(E) \int_0^E (E - E') \phi(E') dE' dE, \quad (4)$$

where  $E_{\max}$  is the maximum beta-ray energy in the decay of interest; e.g., 2.27 MeV for  $^{90}\text{Y}$ . The  $S$  variable is defined in Eq. (1).

The result shown in Eq. (4) has no adjustable parameters. Thus, given the organ-specific absorption value  $\phi(E')$  and the beta spectrum  $P(E)$ , one can in principle compute the organ-to-organ bremsstrahlung radiation dose for any high-energy beta emitter. Moreover, as our knowledge of  $\phi$  values is increased by following photon histories (Monte-Carlo calculations) at various energies and with other organ pairs, it may be possible to estimate dose rates for nonstandard positions

within (e.g., tumors) or outside (e.g., protection sites) the patient's anatomy.

Integrations shown in Eq. (4) were carried out for a number of different target organs and a source in the bladder. Initially, we attempted to fit  $\phi(E')$  as a polynomial in  $E'$  so as to obtain the integrals as mathematical equalities. The complicated variation of the absorbed fraction, however, precluded any simple functional representation. Instead, we used the tabulated  $\phi$  values of Ref (2) and applied a linear photon energy interpolation subroutine to find relevant  $\phi(E')$  magnitudes numerically. The normalized beta spectrum of  $^{90}\text{Y}$  was taken directly from a graphic representation of experimental nuclear data (17). An effective  $\bar{Z}$  of 7 was assumed in the computations.

Numeric accuracy of the resultant  $S$  values was determined by repeating the integrations at different energy step sizes. Convergence was demonstrated by showing that the  $S$  value calculated approached a definite limit as  $dE'$  and  $dE$  approached zero. Typically, energy steps of 0.1 MeV were necessary although, in the bladder as target case, a size of 0.02 MeV was required.

### Dose Measurements

Beside these theoretic estimates, we also measured the brake radiation dose at a number of locations in the male anthropomorphic phantom containing a single  $^{90}\text{Y}$  source in the bladder region. Dosimeters (5 mm diameter by 24 mm long), made of LiF, were calibrated with cesium-137 and cobalt-60 sources which were appropriate to the x-ray energy range required. We also used an outside reading service to corroborate several of the measured doses. This was accomplished by exposing two TLDs at mirror image points within the phantom. One of the dosimeters was read locally, the other sent to the outside service. Tabulated data show the average  $\pm$  the standard deviation of the various readings.

Calibrated sources of purified  $^{90}\text{Y}$ , traceable to the National Bureau of Standards, were provided by a supplier of radiolabeled antibodies. Contamination resulting from  $^{90}\text{Sr}$  was less than three parts per million. An aliquot of 10 to 15 mCi was placed in an empty TLD tube and inserted into the bladder region of the RANDO phantom at slice 33. The bladder area was chosen because it is representative of an abdominal tumor location and  $\phi$  values for a bladder source are available from the MIRD publications (2). An array of up to 30 LiF dosimeters had previously been installed throughout the anatomy of the phantom using the mirror-image strategy described above. The nearest detector was 3 cm away from the beta source so as to preclude measuring any direct beta dose (maximum beta range = 1.0 cm). Dosimeters were exposed to the  $^{90}\text{Y}$  source over a 7- to 10-day period. Exposures were then multiplied by normalizing factors to simulate the result if the decay had been allowed to continue until infinite time. This phantom experiment was repeated three times.

## RESULTS

Calculated bremsstrahlung  $S$  values for a bladder source are shown in Table 1. These were seen to vary over approximately two orders of magnitude between bladder and liver as target organs. Because of the decreasing magnitude of the resultant values, calculations

**TABLE 1**  
Bremsstrahlung S Values and Doses for a Uniform  
Bladder Source of  $^{90}\text{Y}$

Target organ	S value rad/ $\mu\text{Ci-hr}$	Estimated dose <sup>*</sup> mrad/mCi	Measured dose <sup>†</sup> mrad/mCi
Bladder (BL)	$6.7 \times 10^{-6}$	620	$432 \pm 76$ (33)
Uterus (UT)	$1.4 \times 10^{-6}$	130	$260 \pm 60$ (32)
			$71 \pm 4$ (31)
Lower large Intestine	$7.0 \times 10^{-7}$	65	$71 \pm 4$ (31)
Upper large Intestine (ULI)	$1.5 \times 10^{-7}$	14	$47 \pm 10$ (30)
Small Intestine (SI)	$2.1 \times 10^{-7}$	20	$16 \pm 1$ (28)
Kidneys (K)	$2.9 \times 10^{-8}$	2.6	$2.9 \pm 0.3$ (24)
Liver (L)	$1.7 \times 10^{-8}$	1.6	$1.4 \pm 0.7$ (21)

<sup>\*</sup> Doses were calculated using  $\bar{A} = 9.2 \times 10^4 \mu\text{Ci-hr}$ ; i.e., assuming 1mCi of  $^{90}\text{Y}$  and no biologic clearance.

<sup>†</sup> Phantom slice numbers are shown in parentheses.

were not carried out for organs above the level of the stomach. The table also contains estimated and measured doses, in units of mrad/mCi, for the various target organs assuming no biologic clearance of the  $^{90}\text{Y}$  radionuclide.

Several anatomic locations corresponding to RANDO phantom slices were obtained from the planar layout of the MIRD phantom given in Figure 2 of Synder et al. (2). Measured doses shown are averages  $\pm$  s.d. at each slice level. Data values varied over approximately two orders of magnitude with bladder values approaching 0.5 rad/mCi being the maximum recorded. Liver and spleen doses were near 1 mrad/mCi and were the smallest recorded. No significant differences were seen between measurements made in-house or by the commercial reading service.

By graphing the logarithm of the measured dose readings obtained at different slices, one can also estimate an effective half-value layer (HVL). Prior to graphing, all dose measurements were corrected by multiplying by the square of the distance from the source to TLD position so as to take into account the variation caused by the inverse square law. These corrected data are shown in Figure 1 and reveal an effective HVL of  $\sim 15$  cm in the soft-tissue equivalent material at source-detector distances of  $> 5$  cm. Errors shown in the figure indicate the standard deviation.

## DISCUSSION

Calculated organ S values for brake radiation were found to be  $\leq 6.7 \times 10^{-6}$  rad/ $\mu\text{Ci-hr}$  for a source in the bladder. Using the bladder as target organ, one can calculate that the brake radiation dose is only 0.14% of that because of direct beta irradiation (3). Although this ratio is less than Fermi's (1) estimate of 0.81%, it is

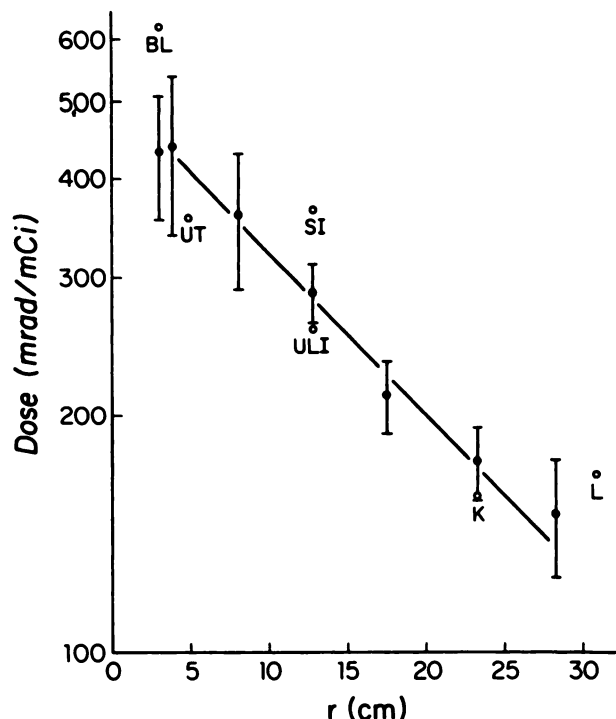


**FIGURE 1**

Brake radiation dose ( $\pm$  s.d.) as a function of distance ( $r$ ) measured from a single source of  $^{90}\text{Y}$  in slice 33 (bladder) of the RANDO phantom. All data (closed circles) are corrected to the 3-cm position using a  $r^2$  multiplier to account for the inverse-square law. Several representative organ dose estimates (open circles) are included with an appropriate inverse-square correction. Organ identifiers are listed in Table 1.

probable that most of the brake rays escape from the bladder without interaction and do not contribute to the local dose. Beta-induced ionizations, on the other hand, are more predominantly delivered within the volume. To relax this constraint somewhat, we may consider the ratio of brake to beta dose when the whole body is the target organ. Using our brake dose estimate of 15 mrad/mCi for  $^{90}\text{Y}$ , the quotient becomes  $5.8 \times 10^{-3}$ —in considerably better agreement with Ref. (1). Theoretic estimates were necessary in this case since we could not measure a representative whole-body dose using TLD methods.

Organ brake radiation dose estimates lay in the range of tens to hundreds of mrad per mCi given a source in the bladder. If we assume the source to be a simulated tumor with a mass of 509 g (2),  $\sim 14$  mCi of  $^{90}\text{Y}$  in the "lesion" would produce a beta dose of 5,000 rad. From our measurements, this amount of activity in the bladder would result in 6 rad bremsstrahlung dose to an organ at 3 cm from the source. If we reduce this distance to the maximum  $^{90}\text{Y}$  beta range of 1 cm, inverse square law estimates result in a tissue dose of at least (neglecting attenuation) 54 rad. While these values are small ( $\leq 1\%$ ) compared to the tumor's beta-ray dose, they are

not negligible and should be considered. It is possible in some tumor geometries; e.g., a colorectal tumor encircling the intestine, that the magnitude of normal gut dose could be higher. An intra-organ dosimetric approach would be more appropriate in such cases, however.

Other indirect effects of a therapeutic beta protocol have been estimated. Leichner et al. (18) have calculated radiation doses of several rad/mCi resulting from blood-borne activity (19). Circulation times were extended in this  $^{90}\text{Y}$  antiferritin example with effective half-times of 9 and 65 hr and weights of 1 and 2, respectively. Thus, circulation times on the order of tens of hours can lead to blood-induced beta radiation doses comparable to those estimated by us for brake radiation and instantaneous uptake. It must be emphasized that relatively long circulation times are not optimal for radiotherapy since a majority of the decays are wasted in the blood with corresponding deleterious effects on normal organs. Molecular engineering of monoclonal tracers would reduce such times appreciably; e.g., a fast compartment half-time as short as 1 hr has been reported (20). It is apparent that bremsstrahlung doses become relatively more important as circulation times are reduced and beta therapy optimized.

Numeric estimates of phantom dose made with Eq. (4) were always found to be within a factor of two of the TLD dosimetry data. The agreement was essentially within the error of measurement (cf Fig. 1) in cases such as the kidneys, upper large intestine and liver whereby the organs were at fixed distances relative to the bladder; i.e., corresponded to a single RANDO slice. For organs occupying several slices, greater care in the analyses was needed prior to comparison with theory.

Lower large intestine extends (2) from the upper large intestine (slice 28) to bladder (slice 33). If we accept the mean position as between segments 30 and 31, the measured value is 59 mrad/mCi in good agreement with our calculation of 65 mrad/mCi. It is clear that this organ exhibits enormous dose variation from 6 mrad/mCi at the ULI to values approaching 400 mrad/mCi near the bladder. Our organ-to-organ dose estimation approach can only give average values in such cases. A similar argument holds for the uterus.

It should be mentioned that the location of the uterus is not given in Snyder et al. (2) so that an anatomy reference (21) was used to determine distance to the bladder. With the approximate value being 2.5 to 3.0 cm, it appeared that slices 31 and 32 were appropriate with 32 being closer to the organ center. The uterus measurement shown in Figure 1 is the average of these two slices.

Calculated bremsstrahlung bladder doses were ~50% higher than the result measured at slice 33 (cf Table 1). It seemed that this difference was directly associated with the short distance between source and detector

since, as shown above, data at greater distances showed considerably better agreement. One must realize that a finite (~1 cm radius) source of  $^{90}\text{Y}$  may not be a good approximation to an extended source of several centimeters diameter which has been assumed for the bladder-to-bladder  $\phi$  value (2). Our data point taken at 3 cm, was, therefore, a sample from within the organ according to the MIRD assumptions and may not be representative of the entire bladder.

It is important to recognize that a point source assumption for our bladder source also leads to overestimation of the dose at 3 cm. Recently, Stabin et al. (22) have utilized a theoretical bremsstrahlung dose equation for a point source of  $^{90}\text{Y}$  in a  $\bar{Z} = 6.8$  material and calculated a value of 600 mrad/mCi at that distance. It thus appeared as if either extended or point source assumptions led to almost identical overestimates near a brake ray source of finite, albeit small, size. It may be that an exact integral over the spatial distribution is necessary in this case.

Measurements of exposures at such short distances can be compared to the earlier protection estimates and measurements (11–13). Using our TLD data, we estimated an exposure rate of  $4.7 \pm 0.8$  mR/hr at 3 cm from a 1-mCi source of  $^{90}\text{Y}$ . This value was in the range of 2.7 to 11 mR/hr previously described with our agreement being best with Berger (12). Measurement of exposure rates near the surface of the phantom revealed a variation between 0.6 and 0.1 mR/mCi/hr at the bladder level (slice 33). As shown in Figure 1, this brake radiation field was quite penetrating with an effective (including scatter) HVL greater than that of  $^{60}\text{Co}$  gamma rays.

## CONCLUSION

We conclude that brake radiation can contribute significant effects to patient dosimetry, particularly at short distances to sources of the high-energy betas. This organ dose can be estimated by the standard MIRD format using an integration over the brake and beta spectra. Agreement in the case of  $^{90}\text{Y}$  was generally good with the best correspondences occurring with those tissues at fixed distances > 5 cm from the bladder source. Organs not in this category—particularly those at very close distances—showed agreement only to within a factor of two of our dose estimation method. Because of the latter consideration and the possibility of a spatially variable distribution of monoclonal antibodies within lesions, we would recommend a smaller-scale approach; e.g., developing a function like that of Stabin et al. (22) for bremsstrahlung dose calculations at relatively small distances. While their methodology is presently based on the assumption of an infinite water medium and is not directly applicable to complicated

practical situations, it offers the essential feature of an explicit dose versus distance relationship.

## ACKNOWLEDGMENTS

The authors thank Dr. Carol Marcus of Harbor-UCLA Medical Center who suggested an evaluation of bremsstrahlung doses. Mr. Michael Stabin of the Radiopharmaceutical Dose Information Center at Oak Ridge Tennessee offered valuable advice throughout the measurements. This investigation was supported by NIH Research Grant Number CA33572 from the National Cancer Institute. The work was made possible in part by support from NIH Research Grant CA43904. Hybritech Inc. of San Diego provided the calibrated samples of purified  $^{90}\text{Y}$ . A preliminary report on these results was given at the Society of Nuclear Medicine 34th Annual Meeting in Toronto.

## REFERENCES

- Orear J, Rosenfeld AH, Schluter RA. Nuclear physics, a course given by Enrico Fermi at the University of Chicago, Revised Edition. Chicago: University of Chicago Press, 1950: 43-47.
- Synder WS, Fisher HL, Ford MR, Warner GG. Estimates of absorbed fractions for monoenergetic photon sources uniformly distributed in various organs of a heterogeneous phantom. *J Nucl Med* 1969; 10 (suppl 3): 5-52.
- Synder WS, Ford MR, Warner GG, Watson SB. "S", Absorbed dose per unit cumulated activity for selected radionuclides and organs. New York: Society of Nuclear Medicine, 1975: 1-257.
- Humm JL. Dosimetric aspects of radiolabeled antibodies for tumor therapy. *J Nucl Med* 1986; 27:1490-1497.
- Order SE, Klein JL, Leichner PK, Frincke J, Lollo C, Carlo DJ. Yttrium-90 antiferritin-a new therapeutic radiolabeled antibody. *Int J Radiat Oncology Biol Phys* 1986; 12: 277-281.
- Ariel IM. Treatment of inoperable primary pancreatic and liver cancer by the intra-arterial administration of radioactive isotopes (Y-90 radiating microspheres). *Ann Surg* 1965; 162: 267-278.
- Mantravadi RVP, Spigos DG, Tan WS, Felix EL. Intraarterial yttrium 90 in the treatment of hepatic malignancy. *Radiology* 1982; 142: 783-786.
- Smith PHS, Thomas PRM, Steere HA, Beatty HE, Dawson KB, Peckham MJ. Therapeutic irradiation of the central nervous system using intrathecal Y-90-DTPA. *Br J Radiol* 1976; 49: 141-147.
- Nemec HW, Fridrich R. Zur Frage der retention und der dosis bei der radiosynovierthese mit yttrium-90-silikatkolloid. *Nuc. Med* 1977; 16: 113-118.
- Kutzner JW, Dahnert T, Schreyer W, Grimm W, Brod KH, Becker M. Yttrium-90 zur Schmerztherapie von Knochenmetastasen. *Nucl Med* 1981; 20: 229-235.
- Cember H. Introduction to health physics, Second Ed. New York: Pergammon Press, 1972: 119.
- Berger MJ. Distribution of absorbed dose around point sources of electrons and beta particles in water and other media. *J Nucl Med* 1971; 12 (suppl 5): 10.
- Bureau of Radiological Health, U. S. Public Health Service, Consumer Protection and Environmental Health Service. *Radiological health handbook*. Washington DC: U. S. Government Printing Office, 1970: 204.
- Loevinger R, Berman M. MIRD Pamphlet No. 1-A schema for absorbed-dose calculations for biologically distributed radionuclides. *J Nucl Med* 1968; 9(suppl 1): 7-14.
- Johns HE, Cunningham JR. The physics of radiology, Third Edition. Springfield, IL: Charles C Thomas, 1969: 52-53.
- Greening JR. Low energy x-ray dosimetry. In: Attix FH, ed. *Topics in radiation dosimetry supplement 1*. New York: Academic Press, 1972:
- Brodsky AB. CRC handbook of radiation measurement and protection section A, volume 1: physical science and engineering data. West Palm Beach, FL: CRC Press, 1978: 425.
- Leichner PK, Nai-Chuen Y, Frenkel TL, et al. Dosimetry and treatment planning for Y-90-labeled antiferritin in hepatoma. *Int J Rad Oncol Biol Phys* 1988; 14: 1033-1042.
- Cloutier RJ, Watson EE. Radiation dose from radioisotopes in the blood. In: *Medical radionuclides: radiation dose and effects (AEC Symposium Series No. 20), CONF 691212*. Oak Ridge, TN, 1970.
- Khaw BA, Yasuda T, Gold HK, et al. Acute myocardial infarct imaging with indium-111-labeled monoclonal antimyosin Fab. *J Nucl Med* 1987; 28: 1671-1678.
- Eycleshymer AC, Schoemaker DM. *A cross-section anatomy*. New York: Appleton-Century-Crofts, 1970: 104-111.
- Stabin MG, Eckerman KF, Ryman JC, Williams LE. Bremsstrahlung dosimetry component in Y-90 monoclonal antibody therapy [Abstract]. *J Nucl Med* 1988; 29: 859.